The Expansion Wave Concept—Part I: Efficient Calculation of Spatial Green's Functions in a Stratified Dielectric Medium

Filip J. Demuynck, *Member, IEEE*, Guy A. E. Vandenbosch, *Member, IEEE*, and Antoine R. Van de Capelle, *Member, IEEE*

***Abstract*—A procedure is given to perform the inverse Fourier transformation relating a spatial Green's function to its spectral equivalent. The procedure is applied to the spectral Green's functions of the double scalar mixed-potential integral expression formulation of the electromagnetic field in a stratified dielectric medium. The extraction technique is used to annihilate every type of "problematic" behavior of the spectral Green's functions. Every annihilating function is inverse Fourier transformed analytically. It is shown that the annihilation of both the surface wave poles and the singularities at the branch point results in a set of analytical spatial functions, which are a very good approximation of the exact spatial Green's function down to relatively small lateral distances. Some very important characteristics of these functions will play a crucial role in Part II of the paper, where a new technique is introduced to model mutual coupling.**

***Index Terms*—Green's functions, nonhomogeneous media.**

I. Introduction

THE possibility to analyze printed structures embedded in a stratified medium containing an arbitrary number of layers is of increasing interest. Especially in space applications, the need to satisfy all sorts of requirements (not only concerning electromagnetic behavior of the structure but also mechanical and thermal behavior) in many cases, can be fulfilled only by using more than one or two layers. Due to the presence of the arbitrary number of layers and due to the need for accuracy, in our view, the most appropriate technique to perform the analysis is to solve a set of integral equations describing the structure using the method of moments. Recently, double scalar mixed-potential integral expressions were formulated for the electric field in a stratified dielectric medium containing an arbitrary number of layers [1]. These general expressions are the basis for corresponding integral equations describing any specific configuration under consideration. They are especially suited to be used in combination with a subsectional expansion scheme in the method of moments. The core of the field expressions is a set of recursively determined spectral Green's functions, which have to be inverse Fourier transformed to obtain their spatial equivalents. This problem is well known and many papers have been published describing procedures to perform this task [4]–[6]. In this paper, however, certain specific properties of the Green's functions will be exploited. First, the expressions for the electromagnetic field due to arbitrary sheet currents are discussed. Second, the efficient calculation procedure will be explained. This procedure will be illustrated in a third section. Finally, the procedure will be compared to what has been published in literature.

Manuscript received September 26, 1994; revised December 29, 1995.

F. Demuynck is with HP-EEsof, Ghent, 9000 Belgium.

G. A. E. Vandenbosch and A. R. Van de Capelle are with the Division ESAT-TELEMIC/Departement Elektrotechniek, Katholieke Universiteit of Leuven, Leuven, B-3001 Belgium.

Publisher Item Identifier S 0018-926X(98)02261-3.

II. Double Scalar Mixed-Potential Integral Equations for the Electromagnetic Field

The general layer configuration is described in [1]. For reasons of simplicity, we will limit ourselves to the case where only sheet currents are present. The tangential electric or magnetic field in layer $i(\vec{F}_{it})$ due to an electric or magnetic sheet current flowing in the transition between layer j and $j+1$ can be written as

$$\begin{aligned}\vec{F}_{it}(x,y,z) = &\int_{x'}\int_{y'} \vec{K}_j(x',y')\ \mathrm{FT}^{-1}(g^K_{ji,F}(\xi,\eta,z))\ dx'\ dy' \\ &+ \vec{\nabla}_t \int_{x'}\int_{y'} (\vec{\nabla}'_t \vec{K}_j(x',y')) \\ &\cdot \mathrm{FT}^{-1}(g^Q_{ji,F}(\xi,\eta,z))\ dx'\ dy' \qquad (1)\end{aligned}$$

where $\vec{K}_j$ is a current derived directly from the sheet current distribution. The inverse Fourier transforms have to be evaluated in $(x-x', y-y')$. The spectral Green's functions for the current $(g^K_{ji,F})$ and the divergence term of the current $(g^Q_{ji,F})$ are derived from the basic TE and TM spectral Green's functions, which are found as the solution of the TE and TM system. It can be verified [1]–[3] that the basic spectral Green's functions for the electric and magnetic field correspond, respectively, to the voltage $(V(\beta,z))$ and the current $(I(\beta,z))$ along the equivalent transmission line circuit shown in Fig. 1. The circuit is excited by either a series unit voltage source $(V_s = 1)$ in the case of a magnetic sheet current or a parallel unit current source $(I_s = 1)$ in the case of an electric sheet current. For each system TE or TM, the following transmission line equations must be fulfilled within each (source free) layer i

$$\frac{d}{dz} I(\beta,z) = -\gamma_i Y_i V(\beta,z) \qquad (2)$$

$$\frac{d}{dz} V(\beta,z) = -\gamma_i Z_i I(\beta,z) \qquad (3)$$

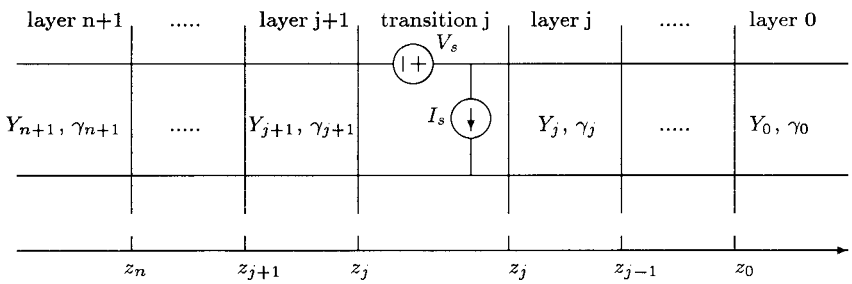

Fig. 1. Transmission line equivalent with sources at transition j.

with $Z_i = 1/Y_i$, and $\gamma_i = \sqrt{(\xi^2+\eta^2)-k_i^2} = \sqrt{\beta^2-k_i^2}$. Y_i equals $\gamma_i/j\omega\mu_i$ for the TE system and $j\omega\epsilon_i/\gamma_i$ for the TM system, respectively. These equations can be solved making use of the appropriate boundary conditions at the transitions between the layers and at infinity.

III. Efficient Calculation of the Green's Functions

It is well known that in multilayered structures most Green's functions can be derived analytically in the spectral domain. Their spatial equivalents can be calculated using an inverse Fourier transformation. If $g(\xi,\eta)$ is a spectral Green's function and $G(x,y)$ its spatial equivalent, then the relation between them is given by

$$G(x,y) = \frac{1}{4\pi^2}\int_\xi\int_\eta g(\xi,\eta)\,e^{-j(\xi x+\eta y)}\,d\xi\,d\eta. \tag{4}$$

After a transformation from Cartesian into cylindrical coordinates given by $x = r\cos\phi$, $y = r\sin\phi$, $\xi = \beta\cos\delta$, and $\eta = \beta\sin\delta$ and making use of the fact that only spectral Green's functions independent of δ are considered, we obtain a Sommerfeld type integral

$$G(r) = \frac{1}{2\pi}\int_0^\infty \beta g(\beta)J_0(\beta r)\,d\beta \tag{5}$$

with J_0 the Bessel function of the first kind and of order zero. The latter equation expresses that for spectral Green's functions only depending on β, the corresponding spatial Green's functions only depend on the lateral separation r between source and observation point. The integral can be regarded as an integral in the complex plane. This means that the integration contour may be deformed. However, our procedure disregards this possibility and integrates over the positive real axis.

A. The General Procedure

If the spatial Green's function is evaluated very close to the source (r is small), the oscillation period of the Bessel function is very large and the behavior of the spatial Green's function is mainly determined by the asymptotic behavior for large arguments of $\beta g(\beta)$. The integrand may decrease very slowly, resulting in an unacceptable convergence of the integral in terms of the upper integration limit. On the other hand, far away from the source (r is large), the oscillation period becomes very small. If $\beta g(\beta)$ is slowly varying, the contribution to the integral is small because within one period of the oscillation, the positive part is annihilated by an almost equal negative part. Only rapid variations, which occur where the derivative of $\beta g(\beta)$ becomes large, can give a substantial contribution to the integral. This is especially true at the surface wave poles and at the branch point ($\beta = K$, K is the wave number of the open half-space). There the derivatives become infinite. Both problems are illustrated in Fig. 2. The solution to both problems consists of subtracting a well-chosen analytic function showing the behavior needed to eliminate the difficulty in question and re-adding the same function after analytical inverse Fourier transformation. The remaining smooth spectral function will contribute substantially at intermediate values of r only.

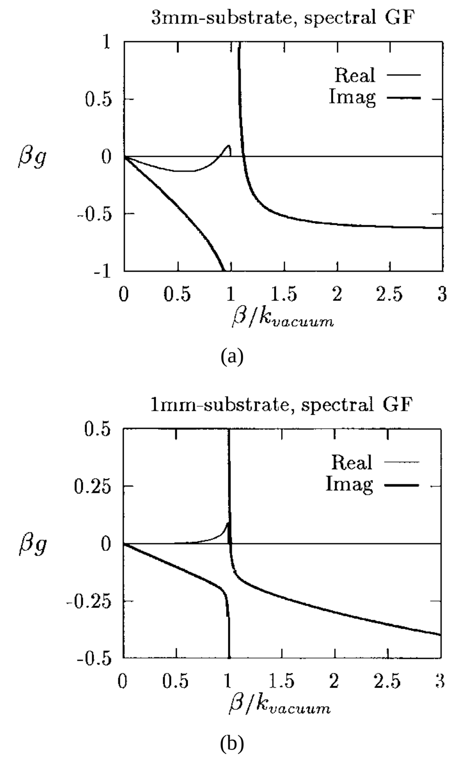

Fig. 2. Product of β and spectral Green's function for the transversal electric field in a layer structure consisting of a substrate backed by a ground plane. Source: divergence term of electric sheet current in air–substrate interface; observation point in the same layer interface; frequency = 10 GHz. (a) Substrate 1: thickness = 3 mm, $\epsilon_r = 2$, $\tan\delta = 0$. (b) Substrate 2: thickness = 1 mm, $\epsilon_r = 2$, $\tan\delta = 0$.

1) Contributions of the Asymptotes: The asymptotic behavior of $\beta g(\beta)$ for large β determines the contribution in the immediate neighborhood of the source. The decay of $\beta g(\beta)$ is very slow and a function $\beta g_a(\beta)$ multiplied by a proper

TABLE I
ANNIHILATING SPECTRAL FUNCTIONS AND THEIR SPATIAL EQUIVALENTS FOR THE ASYMPTOTES

n	$g_a(\beta)$	$G_a(r)$
0	$e^{-\beta\Delta}$	$\delta(r)$ if $\Delta = 0$ $\frac{\Delta}{2\pi(\sqrt{\Delta^2+r^2})^3}$ if $\Delta \neq 0$
1	$\frac{1-e^{-\beta t}}{\beta}e^{-\beta\Delta}$	$\frac{1}{2\pi}\left(\frac{1}{\sqrt{\Delta^2+r^2}} - \frac{1}{\sqrt{(\Delta+t)^2+r^2}}\right)$
2	$\frac{(1-e^{-\beta t})^2}{\beta^2}e^{-\beta\Delta}$	$-\frac{1}{2\pi}\ln\frac{(\Delta+\sqrt{\Delta^2+r^2})(\Delta+2t+\sqrt{(\Delta+2t)^2+r^2})}{(\Delta+t+\sqrt{(\Delta+t)^2+r^2})^2}$

constant C_a is subtracted to improve the convergence of the integration. If g_a is chosen properly, the contribution above a threshold $\beta_{\max}$ can be neglected. This function has to be chosen so that it can be re-added after analytical integration. It is calculated using the same recursive procedure as to calculate the original spectral Green's function [1], but taking into account that β is much larger than the real part of any wave number of a dielectric layer in the structure and systematically keeping only the slowest decaying exponential function throughout the recursive calculation. The physical interpretation of this last operation is that at high values of β, a very good approximation of the exact Green's function can be obtained by considering only the direct wave between source and observation point. Reflected waves (reflected at the transitions) always are much smaller because the exponential decay depends on the total distance traveled. Since only the slowest decaying exponential function (the direct wave) is kept in g_a—the slowest—but one decaying exponential function can be used as a measure for the relative error made by truncating the integration interval. The maximum relative error made for the entire layer structure depends on $e^{-2\beta_{\max}\Delta_{\text{thin}}}$, where Δ_{thin} is the thickness of the thinnest dielectric layer adjacent to any sheet current source in the structure. This can be used to determine $\beta_{\max}$. The spectral Green's functions for large β are proportional to $\beta^{-n}e^{-\beta\Delta}$ with $n = 0, 1,$ or 2. Δ is the z separation between source and observation point measured along the z axis. For each n, the annihilating spectral function and its spatial equivalent can be found in Table I. The parameter $t = 1/k_{\max}$, $k_{\max}$ is the maximum wave number in the layer structure is introduced to avoid a singularity at the origin of the spectral function. The spatial functions have a singularity (which can be integrated) for $r = 0$ and $\Delta = 0$.

2) Contributions of the Singularities: The singular behavior of $\beta g(\beta)$ determines the contribution further away from the source. The three types of problematic behavior that matter can be described by the function $C(\beta^2 - S^2)^n$ with S the problematic β point, C a complex constant, and n equal to -1 at a surface wave pole and equal to -0.5 or $+0.5$ at the branch point. For each type of singularity, a new function is proposed to annihilate the singular behavior of the integrand. These functions are chosen very carefully for several reasons: 1) the behavior of the function in the neighborhood of the singularity should coincide with the behavior of the Green's function; 2) the inverse Fourier transform of the function should be known analytically; and 3) the introduction of a new asymptote for large β should be avoided since this affects the truncation procedure described in the previous section. In the case of a thick substrate, the contribution due to the surface wave pole will dominate very rapidly and is sufficient as approximation for a spatial Green's function at larger distances. However, it will be shown that for electrically thin structures, where the surface wave pole is located close to the branch point, it is necessary to annihilate the singular behavior of both the surface wave pole and the branch point. Subtracting both will result in an analytically calculated approximation for the Green's function, which is acceptable down to much lower distances than what is obtained when the pole only is subtracted.

Surface wave pole singularities: The physical interpretation of a pole is that it determines an eigenmode of the layer structure. The numerical test to locate a pole is based on the eigenmode condition. The residue of a Green's function at a pole can be calculated by analyzing the functional behavior in the immediate neighborhood of the pole and comparing it to the behavior of $R/(\beta - P)$. In [3], some interesting properties of the surface waves were proven: 1) the z dependence of the surface wave fields follows the source-free transmission line equations and, as a consequence, is unique (independent of the source location); 2) surface wave modes of the same type (either TE or TM) are orthogonal along the z direction; and 3) space and surface wave fields are orthogonal along the z direction. Due to the uniqueness of the surface wave field, the residue at the pole P of a Green's function g for a field component of the electromagnetic field F due to a source S_j can be written as a product of a z-dependent function and a source dependent constant

$$R(z) = \lim_{\beta \to P}(\beta - P)g_{j,F}(\beta, z) = C^{F,P,-1}(z)C_j^{P,-1} \qquad (6)$$

with $g_{j,F}(\beta, z)$ equal to $V(\beta, z)$ or equal to $I(\beta, z)$, depending on which field component is considered. The behavior of the spectral Green's function in the proximity of a surface wave pole P can be annihilated by subtracting a spectral function $c^{P,-1}(\beta)$

$$c^{P,-1}(\beta) = 2P\left(\frac{1}{\beta^2 - P^2} - \frac{1}{\beta^2 + P^2}\right) = \frac{4P^3}{\beta^4 - P^4}. \qquad (7)$$

The first part of $c^{P,-1}$ shows the equal behavior around the singularity; the second part makes the decay of the resulting function $c^{P,-1}$ large enough (faster than $1/\beta^2$) to avoid the introduction of a new spectral asymptote and, thus, a new singularity at the origin in the spatial domain. The corresponding spatial function can be calculated analytically

$$\begin{aligned} C^{P,-1}(r) &= \frac{1}{2\pi}\int_0^\infty \beta c^{P,-1} J_0(\beta r)\, d\beta \\ &= -\frac{jP}{2}(H_0^{(2)}(Pr) - H_0^{(2)}(-jPr)). \end{aligned} \qquad (8)$$

One can easily verify that this spatial function is smooth when r tends to zero. The expansion of $C^{P,-1}(r)$ for larger r results in

$$C^{P,-1}(r) \simeq -jP\frac{e^{j\pi/4}}{\sqrt{2\pi}}\frac{e^{-jPr}}{\sqrt{Pr}}, \qquad |Pr| \gg 1 \qquad (9)$$

which is the well-known behavior for surface waves at larger r.

Branch point singularities: For half-open structures, a second type of singularity occurs at the branch point $\beta = K$ with K the wave number of the open half space. The Green's functions can be expanded in series around $\gamma = \sqrt{\beta^2 - K^2} = 0$ resulting in (the proof is beyond the scope of this paper)

$$g_{j,F}(\beta, z) = A_{-1}^F(z)\frac{1}{\gamma} + A_0^F(z)\frac{1}{K} + A_1^F(z)\frac{\gamma}{K^2} + A_2^F(z)\frac{\gamma^2}{K^3} + \cdots. \tag{10}$$

The behavior which causes an infinite derivative is proportional to $(\beta^2 - K^2)^n$ with either $n = -0.5$, $n = +0.5$, or both. The behavior with $n = -0.5$ can only occur if all the layers have identical dielectric properties. This is the homogeneous case, which means that there are no poles. The behavior with $n = +0.5$ exists in all types of planar structures, homogeneous or not.

First, the nonhomogeneous layer structures are considered where n equals $+0.5$ for the dominant singular behavior at the branch point ($A_{-1}^F = 0$). The problem behavior can be annihilated using $c^{K,+0.5}(\beta)$

$$c^{K,+0.5}(\beta) = \frac{1}{K^2}\left(\sqrt{\beta^2 - K^2} - \beta + \frac{K^2}{2\sqrt{\beta^2 + K^2}}\right). \tag{11}$$

The first part of $c^{K,+0.5}$ is necessary to annihilate the singular behavior. The rest ensures that for large β the decay is large enough to avoid the introduction of a spatial singularity at the origin. The inverse Fourier transform can be calculated analytically

$$C^{K,+0.5}(r) = \frac{K}{2\pi}\left(-\left(\frac{1}{(Kr)^3} + j\frac{1}{(Kr)^2}\right)e^{-jKr} + \frac{1}{(Kr)^3} + \frac{1}{2Kr}e^{-Kr}\right). \tag{12}$$

One can easily verify that this spatial function is smooth when r tends to zero. The expansion of $C^{K,+0.5}(r)$ for larger r results in

$$C^{K,+0.5}(r) \simeq -jK\frac{1}{2\pi}\,\frac{e^{-jKr}}{(Kr)^2}. \tag{13}$$

This r^{-2} contribution will be part of the space wave launched in the direction parallel to the layer structure. Consequently, a zero in the far field can be observed in directions close to the ones parallel with the layer structure for a nonhomogeneous structure. In the Appendix, a very important property is proven: "the z dependence of this part of the space wave follows the source-free transmission line equations and, as a consequence, is unique (independent of the source location)." Consequently, at the branch point K of a Green's function g for a field component of the electromagnetic field F due to a source S_j, one can write

$$A_1^F(z) = \lim_{\beta \to K}\frac{K^2}{2}\,\frac{d^2}{d\gamma^2}(\gamma g_{j,F}(\beta, z)) = C^{F,K,+0.5}(z)C_j^{K,+0.5} \tag{14}$$

where $g_{j,F}(\beta, z)$ equals $V(\beta, z)$ or $I(\beta, z)$, depending on which field component is considered.

In principle, the problem is solved. However, if a pole P is located in the immediate neighborhood of the branch point K, the use of the function $c^{K,+0.5}$ causes a problem. This is illustrated in Fig. 4(a), where a spectral function is depicted after extraction of the problematic behavior. Although the infinite derivative at K has disappeared, the derivative is still quite large around K. The consequence can be seen in the spatial domain [Fig. 4(b)]: the numerical integration is necessary up to large distances ($\gg 2.6\lambda_{\text{vacuum}}$) and the integration technique should be able to handle rapid variations of the integrand to avoid the oscillations. It is clear that this has to be avoided. The problem can be solved in an elegant way by using a subtraction function based on a special expansion in series around $\gamma = 0$ of $g_{j,F}(\beta, z)$. It is easily proven that every Green's function can be written as

$$g_{j,F}(\beta, z) = \frac{D_0 + D_1\gamma + D_2\gamma^2 + \cdots}{E_0 + E_1\gamma + E_2\gamma^2 + \cdots}, \qquad \beta \simeq K. \tag{15}$$

In the immediate neighborhood of K, only the first two expansion terms have to be considered. Taking this into account together with the singular behavior around the pole and the branch point, (15) can be worked out yielding an approximation for the singular behavior of the function g

$$g_{j,F}(\beta, z) \simeq R\frac{2P}{\beta^2 - P^2} + R\frac{P/\gamma_p}{\gamma + \gamma_p} + (A_1^F/K^2 + RP/\gamma_p^3)\gamma, \qquad \beta \simeq K \tag{16}$$

where $P = \sqrt{K^2 + (E_0/E_1)^2}$, $R = -2(E_0/E_1)\,(-(D_1E_0)/E_1^2 + D_0/E_1)$, and $\gamma_p = -(E_0/E_1) = \sqrt{P^2 - K^2}$ with P, K, R, and A_1^F known. Consequently, the singular behavior of the Green's function can be approximated by

$$g_{j,F}(\beta, z) \simeq C^{F,P,-1}(z)C_j^{P,-1}\left(\frac{2P}{\beta^2 - P^2}\right) + C^{F,K,-0.5}(z)C_j^{K,-0.5}\left(\frac{1}{\gamma + \gamma_p} + \frac{\gamma}{\gamma_p^2}\right) + C^{F,K,+0.5}(z)C_j^{K,+0.5}\left(\frac{\gamma}{K^2}\right), \qquad \beta \simeq K \tag{17}$$

with $C^{F,K,-0.5}(z) = C^{F,P,-1}(z)$ and $C_j^{K,-0.5} = C_j^{P,-1}P/\gamma_p$. It is clear that the problem caused at the pole can be annihilated in the same way as before with $c^{P,-1}$. The problem caused at the branch point K can be annihilated by using the function $c^{K,+0.5}$ for the third term and a new function $c^{K,-0.5}$ for the second term

$$c^{K,-0.5} = \frac{1}{\sqrt{\beta^2 - K^2} + \gamma_p} - \frac{1}{\sqrt{\beta^2 + K^2}} + \frac{K^2}{\gamma_p^2}c^{K,+0.5}(\beta). \tag{18}$$

The inverse Fourier transform of $1/(\gamma+\gamma_p)$ is calculated approximately. If the pole is located close to the branch point (which is the case), γ_p is small and $1/(\gamma+\gamma_p)\simeq 1/\gamma$ over the whole spectral region except in the immediate neighborhood of the branch point. After expansion of $1/(\gamma+\gamma_p)$ in series around K, the exact singular behavior very close to the branch point (which determines the spatial dependence at higher r values) is proportional to $-\gamma/\gamma_p^2$. Using

$$\frac{1}{2\pi}\int_0^\infty \frac{\beta J_0(\beta r)}{\gamma}d\beta = -jK\frac{e^{j\pi/2}}{2\pi}\,\frac{e^{-jKr}}{Kr} \tag{19}$$

and

$$\frac{1}{2\pi}\int_0^\infty \frac{\beta\gamma J_0(\beta r)}{\gamma_p^2}d\beta = -\frac{K^3}{\gamma_p^2}\,\frac{e^{j\pi/2}}{2\pi}\,\frac{e^{-jKr}}{(Kr)^2}\left(1-\frac{j}{Kr}\right) \tag{20}$$

one can verify that the spatial function $C^{K,-0.5}$ can be approximated in an excellent way by the following function:

$$C^{K,-0.5}(r)\simeq -jK\frac{e^{j\pi/2}}{2\pi}\left(\frac{e^{-jKr}}{Kr}\left(\frac{1}{1-j\left(\frac{\gamma_p}{K}\right)^2Kr}\right) - \frac{e^{-Kr}}{Kr}\right)+\frac{K^2}{\gamma_p^2}C^{K,+0.5}(r). \tag{21}$$

The expansion of the first term of $C^{K,-0.5}(r)$ for larger r is first proportional to e^{-jKr}/Kr and then for even larger r, depending on γ_p/K, proportional to $e^{-jKr}/(Kr)^2$. The expansion of the second term is already given above.

Second, in homogeneous structures, n equals -0.5 for the dominant singular behavior at the branch point. This singular behavior is annihilated using the first term of $c^{K,-0.5}(\beta)$ with $\gamma_p = 0$. The expansion of $C^{K,-0.5}(r)$ for larger r is then proportional to e^{-jKr}/Kr. This r dependence is part of the space wave launched by an impulse source in a homogeneous structure in the direction parallel to the ground plane. $c^{K,+0.5}(\beta)$ and $C^{K,+0.5}(r)$ are used for the contribution with $n = +0.5$.

3) The Numerical Integration: After the removal of the singularities and the asymptote of the spectral Green's function, a smooth function is obtained. Its contribution to the spatial Green's function is calculated numerically. The integration interval is divided into N equal subintervals ($\Delta\beta = \beta_{\max}/N$) where the Bessel function is approximated by a third degree polynominal and the smooth function by a first degree polynominal. The integration over each subinterval is done analytically and the contributions are summed.

B. Approximation at High r Values (Above $r_{\max}$)

Due to the rapid decrease of the asymptotic contributions and the numerically calculated contributions, in general, every spatial Green's function $G_{j,F}$ for component F of the electromagnetic field due to a source S_j evaluated not too close to the source can be approximated as

$$\begin{aligned} G_{j,F}&(x-x',y-y',z)\\ &\simeq \sum_{P^{\rm TM}} C^{F,P^{\rm TM},-1}(z)C^{P^{\rm TM},-1}(R)C_j^{P^{\rm TM},-1}\\ &\quad + C^{F,K^{\rm TM},-0.5}(z)C^{K^{\rm TM},-0.5}(R)C_j^{K^{\rm TM},-0.5}\\ &\quad + C^{F,K^{\rm TM},+0.5}(z)C^{K^{\rm TM},+0.5}(R)C_j^{K^{\rm TM},+0.5}\\ &\quad + \sum_{P^{\rm TE}} C^{F,P^{\rm TE},-1}(z)C^{P^{\rm TE},-1}(R)C_j^{P^{\rm TE},-1}\\ &\quad + C^{F,K^{\rm TE},-0.5}(z)C^{K^{\rm TE},-0.5}(R)C_j^{K^{\rm TE},-0.5}\\ &\quad + C^{F,K^{\rm TE},+0.5}(z)C^{K^{\rm TE},+0.5}(R)C_j^{K^{\rm TE},+0.5} \end{aligned} \tag{22}$$

where $P^{\rm TM}$, $P^{\rm TE}$, and $K^{\rm TE} = K^{\rm TM} = K$ are the dominant TM-poles, the dominant TE-poles, and the branch point, respectively, $R=\sqrt{(x-x')^2+(y-y')^2}$ and

$$C^{P^{\rm TM/TE},-1}(R)\sim e^{-jP^{\rm TM/TE}R}/\sqrt{P^{\rm TM/TE}R} \tag{23}$$

$$C^{K^{\rm TM/TE},-0.5}(R)\sim e^{-jKR}/(KR) \text{ or } e^{-jKR}/(KR)^2 \tag{24}$$

$$C^{K^{\rm TM/TE},+0.5}(R)\sim e^{-jKR}/(KR)^2. \tag{25}$$

Consequently, the electromagnetic field evaluated in the layer structure not too close to the source is composed of a set of waves: a number of surface waves and the part of the space wave launched in the direction of the ground plane. The r dependence and z dependence of each wave is known analytically and is unique, independent of the source S_j. Currents of a different type (magnetic or electric) flowing in different transitions and with a different shape all excite the same waves, each with its own excitation coefficient C_j.

The threshold above which this approximation is used is called $r_{\max}$. In the section with the numerical results, it will be illustrated that this threshold can be reduced down to values around 0.05 $\cdots$ 0.15$\lambda_{\rm vacuum}$. This implicates that coupling between, e.g., antennas, can be described with analytically known Green's functions. This very important property will be used in the second part of the paper where the expansion wave concept is introduced.

IV. Numerical Results

The procedures developed and the problems which led to these procedures can be illustrated.

First, the necessity to extract the branch point singularity for electrically thin structures is illustrated. The structure consists of a substrate with relative permittivity 2, backed by a perfectly conducting ground plane. The frequency is 10 GHz. Consider the transversal electric field on top of the substrate generated by an arbitrary electric sheet current in the same layer interface. The product of β and the spectral Green's function of this field for the divergence term of the current is given in Fig. 2 for two substrate thicknesses, respectively, 3 and 1 mm. The function goes to a constant for high values of β and both a pole and the branch point can be observed. The modified spectral function obtained by applying the techniques of asymptotic extraction and extraction of the

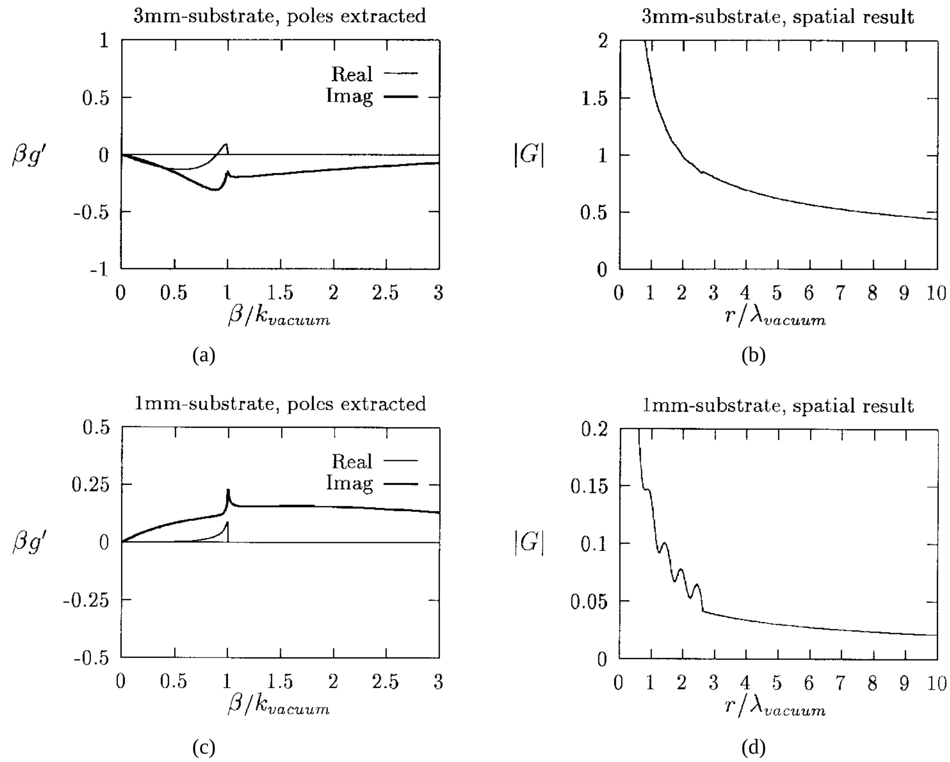

Fig. 3. Spectral function of Fig. 2 after asymptotic extraction and pole extraction and corresponding spatial Green's function (numerical integration up to $r_{\max} \simeq 2.6\lambda_{\text{vacuum}}$).

poles and the resulting spatial Green's function are given in Fig. 3. For both thicknesses, the spectral function now goes to zero for large β and the pole has vanished. However, it is clearly shown in Fig. 3(b) and (d) that the extraction of the asymptote and pole alone only yields excellent results for thick substrates. The ripples and the discontinuity at $r_{\max}$ (which is chosen $\simeq 2.6\lambda_{\text{vacuum}}$) in the spatial Green's function for the thin substrate are caused by the square root behavior near the branch point. Both can be removed by decreasing $\Delta\beta$ and by increasing $r_{\max}$ at the cost of a higher calculation time! Although in principle, these phenomena also occur for thick substrates, they can hardly be observed in these cases due to the presence of a dominating pole. Two techniques to annihilate the singularity around the branch point, which is necessary for the thin 1-mm substrate, are considered. Technique 1 only uses $c^{K,+0.5}$; technique 2 makes use of both $c^{K,+0.5}$ and $c^{K,-0.5}$. The results for both techniques are given in Fig. 4. It is shown that technique 1 even worsens the problem. The derivative at the branch point is now finite but very large (this can be seen if the plot is zoomed in at the branch point). A very large variation in the modified spectral Green's function is introduced, which makes the numerical integration necessary up to very large distances. Consequently, one would expect that a decrease of $\Delta\beta$ and an increase of $r_{\max}$ are necessary $\cdots$. However, technique 2 solves the problem completely. The modified Green's function is very smooth, $\Delta\beta$ can be chosen rather high without introducing the ripple problem, and $r_{\max}$ can be reduced. In the calculations the following numerical parameters were used: $\beta_{\max}\Delta_{\text{thin}} = 6$, $\Delta\beta = 10$, and $r_{\max} = \pi/(4\Delta\beta)$ [at the discontinuity in the spatial functions in Figs. 3(b), 3(d), and 4(b)].

Second, the results obtained by using the approximation for high r values are compared with the results of the general procedure. Some commercially available substrates are used in the examples. First, four RT/duroid substrates are compared: two low permittivity substrates (RT/duroid 5880, $\epsilon_r = 2.2$, $\tan\delta = 0.0009$) with a thickness of respectively 0.38 and 1.57 mm and two high-permittivity substrates (RT/duroid 6010, $\epsilon_r = 10.2$, $\tan\delta = 0.0024$) with a thickness of, respectively, 0.25 and 1.27 mm. The frequency is 10 GHz. The influence of the substrate thickness and the dielectric constant is investigated. The numerical parameters are the same as in the previous case. It is clearly demonstrated [Fig. 5(a)–(d)] that the analytical contributions of the space and surface wave dominate down to relatively small distances, about 0.05 $\cdots$ $0.15\lambda_{\text{vacuum}}$, depending on the thickness and the permittivity of the substrate. Consequently, $r_{\max}$ can be reduced down to this value. Without the extraction of the branch point singularity, $r_{\max}$ should be increased to a distance where the contribution due to the pole dominates. This is strongly dependent on the substrate thickness and the permittivity. The contribution due to the branch point would become part of the numerically inverse Fourier transformed function. This contribution represents the part of the space wave launched in the directions parallel to the ground plate. This part cannot be neglected for coupling between antennas in the case of the relatively thin structures (γ_p/K is small) where the surface wave doesn't dominate the space wave contribution. A second example is a very low permittivity two-layer structure. On the ground plane lies a sheet of Eccofoam (fabricated by Emerson & Cuming) with $\epsilon_r = 1.03$ and a thickness 6.35 mm. On top of this lies a sheet of 3M Cu Clad with $\epsilon_r = 2.17$,

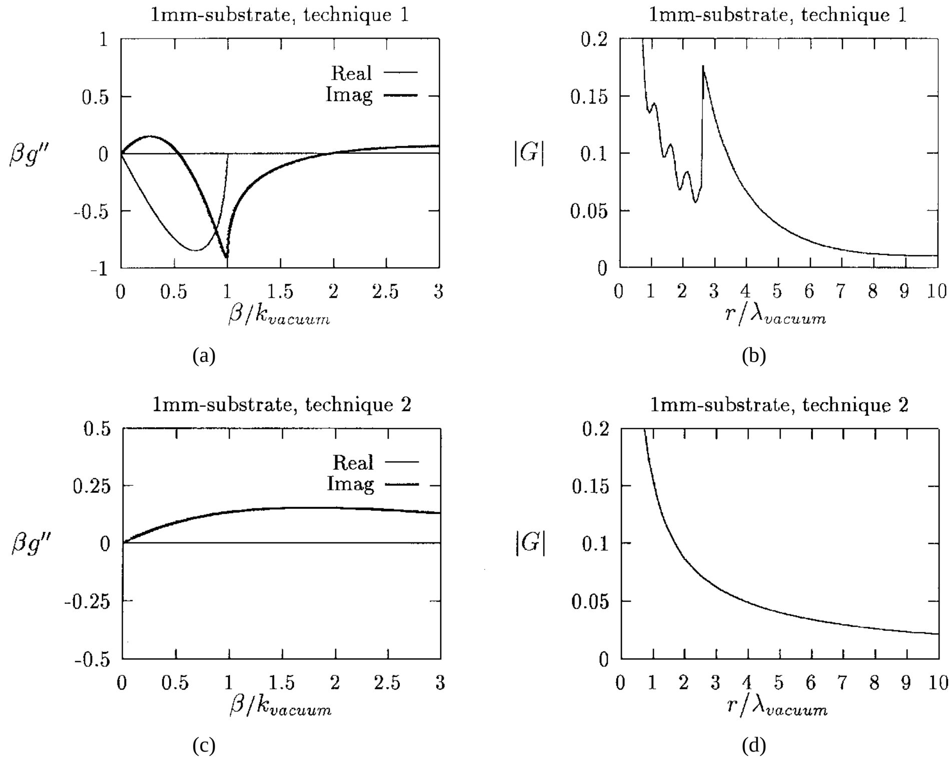

Fig. 4. Spectral function of Fig. 3, substrate thickness 1 mm after branch point extraction, and corresponding spatial Green's function. Top: technique 1—use of $c^{K,+0.5}$ only. (a) Spectral. (b) Spatial; bottom: technique 2—use of both $c^{K,+0.5}$ and $c^{K,-0.5}$. (c) Spectral. (d) Spatial (numerical integration up to $r_{\max} \simeq 2.6\lambda_{\text{vacuum}}$).

$\tan\delta = 0.0009$, and a thickness of 0.5 mm. The frequency is 3.3 GHz. The influence of the surface wave in this quasi-homogeneous structure is negligible [Fig. 5(e)]. The results are very close to the calculations with a perfectly homogeneous substrate.

The exact calculation time depends on the numerical parameters used and, of course, on the computer .... Our calculations are made with a DECstation 5000/240. For the structure of Fig. 5(b) ($\beta_{\max} = 4000$, evaluated in 400 β points, and evaluated in 200 r-points), the calculation of the spectral Green's function takes 0.80 s, the inverse Fourier transformation 0.35 s.

The most important result is the fact that the dominant contributions to the Green's functions proportional to $1/\sqrt{r}$, $1/r$, and $1/r^2$, are calculated analytically. They can be used as an excellent approximation down to very low distances to the source. Together with the use of the properties proven in the Appendix for this part of the space wave and in [3] for the surface waves, it allows to describe mutual coupling between antennas in a new very elegant way. This is the scope of the second part of the paper.

V. Discussion

In this section, each step of the procedure is examined in relation to what has been published in literature. The first fundamental choice made is to use a space-domain formulation of the electromagnetic field. This allows us to work with spectral Green's functions having a dependency only on β, which results in spatial Green's functions only dependent on r [1]. In this way, the double infinite spectral integration [8] is avoided. The spectral integration can be reduced into an integration only over β. The convolution of a Green's function with the corresponding source function is calculated in the spatial domain, which is an easy task if a subsectional expansion scheme is used. A big advantage of the space-domain formulation is the possibility to change the nature of the source function after the calculation of the spatial Green's functions. It is thus most efficient to store a Green's function after its computation and to recall it whenever necessary. Both the spatial and the spectral formulation are used in literature, for example, the first one by Mosig and Gardiol in [7] and the latter one by Pozar in [9] and [10].

For low r, the reduction of the integration domain is necessary because the decay of the integrand is too low, introducing a spatial singularity at the origin. It is well known that this can be solved by using asymptotic extraction techniques. For specific layer geometries in some cases very efficient asymptotic functions can be found in literature. An example is the two-layer case backed by a conducting ground plane described in [4] and [5]. The asymptotic functions given in [7] even allow a complete near-field approximation. In a multilayered structure with magnetic and/or electric sheet current sources, a generalized technique has to be used as the one presented here.

The presence of singularities in the integrand can be treated in several ways. The first one is to choose a different path in the complex β plane. This can be done directly as in [6] or, in some cases, using the technique of [7], where eventually no singularities arise in the functions to be integrated. The second way is to use an extraction technique, the solution chosen in

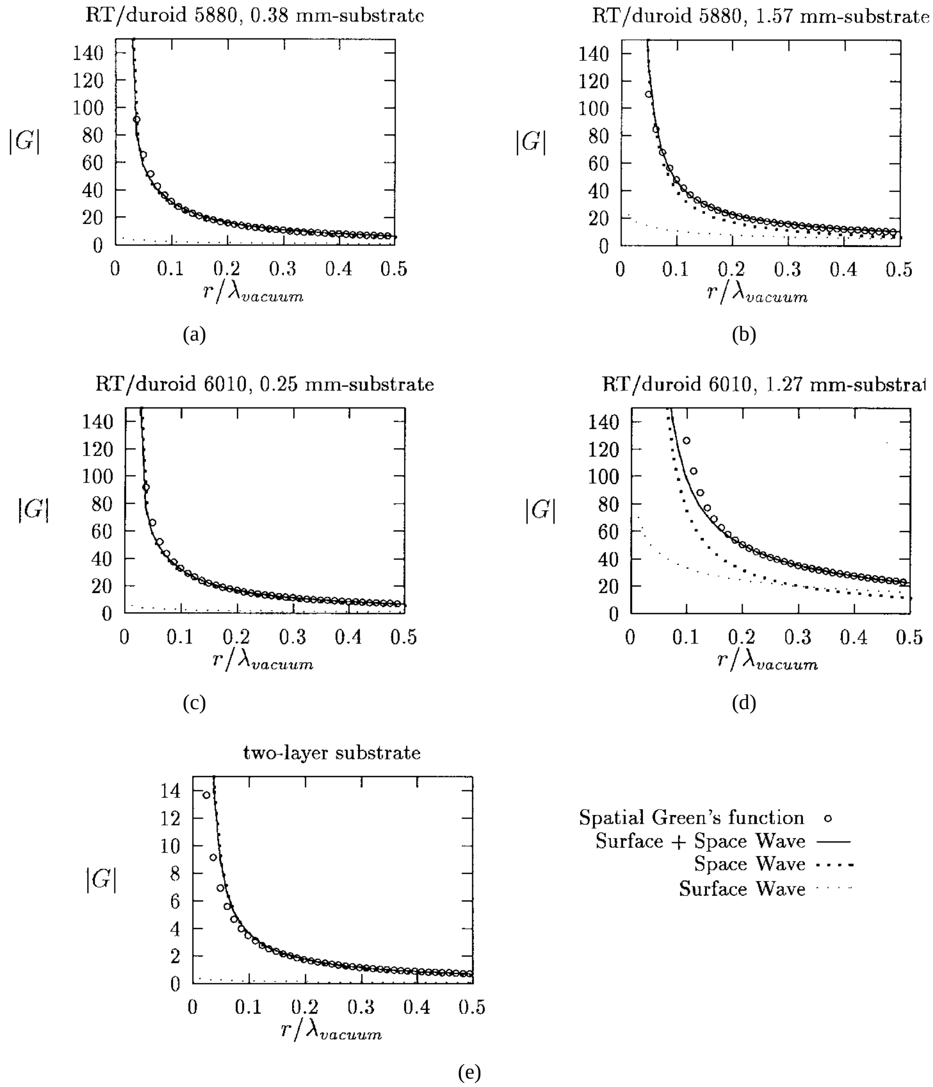

Fig. 5. Spatial Green's function for the transversal magnetic field for different substrates. Source: magnetic sheet current on top of the ground plate, observation point in the same layer interface; circles: spatial Green's function taking all contributions into account; solid line: approximation taking the space and surface wave contributions into account only; thick dots: space wave contribution; thin dots: surface wave contribution.

this work, and in [4] and [5] for the poles. Choosing a different path also solves the problem of the branch point. However, if one prefers to perform the integration along the real axis, a change of variables [5] or, again, an extraction technique can be used to solve the branch-point problem. Although changing the integration path is very popular, in our view the integration along the real axis combined with the unique extraction technique presented here, clearly has advantages. The main advantage is certainly the possibility to express the Green's functions, evaluated not too close to the source as a sum of simple analytical functions with a well-known physical meaning: surface waves and the dominant parts of the space wave. It is important to emphasize that in our technique only rapid variations on the real axis have to be taken into account. Concerning poles, this implicates that only poles on the real axis or in the immediate neighborhood of the real axis have to be located. These poles correspond to surface waves that really propagate without losses or with small losses, respectively. Poles away from the real axis corresponding to exponentially decreasing waves do not have to be taken into account and, thus, do not have to be located. In most practical cases, even in cases involving layer structures with many layers, this means that at most only a few poles have to be located. From the reasoning followed, it is clear that missing one of these poles can only be allowed if its contribution is negligible compared to the contributions of the other singularities (both poles and branch point). Since the ease to locate a pole is proportional to its contribution, using an appropriate technique it is relatively simple to find all the relevant poles in a calculation time negligible compared to the overall calculation time.

The characteristics of the waves used open an opportunity to model mutual coupling in a very elegant way, the scope of the second part of the paper. To our knowledge, this paper is the first one that treats branch points in much the same way as poles. Our subtraction functions clearly differ from the ones used by other authors [4], [5]. In our view, they are very appropriate since they lead to an unique procedure working for all r values. The terms proportional to $1/\sqrt{r}$, $1/r$, and $1/r^2$ are known in an analytical way. Even at relatively small values of r, this contribution yields excellent results. This is due to the extraction of the branch point singularities. Consequently, a lot of computational effort can be saved.

Concerning the correctness and the accuracy of the global procedure, we refer to the agreement between calculated and measured results for the antenna structures given in [1] and [11] for which the Green's functions were calculated with the procedure given in this paper and to the second part of the paper. Concerning the efficiency of the procedure, it has to be emphasized that most of the techniques described in this paper only take a small amount of calculation time: the asymptotes and the constants C_j and the functions $C^F(z)$ for poles and branch point are all calculated using the recursive technique of [1]. The numerically calculated part of the inverse Fourier transform has to be determined for low r values only.

Recently, two very interesting papers were published concerning the problem of calculating the spatial Green's function as the inverse Fourier transform of its spectral equivalent. In [12], a complete set of asymptotic closed-form microstrip surface Green's functions based on the power series expansion of the spectral Green's functions of the two-layer system backed by a conducting ground plane is given. In [13], the technique is extended to the case of a three-layer structure backed by a ground plane. Unfortunately, the authors argue that their method does not seem to be readily applicable to arbitrary Green's functions in multilayered dielectric structures.

VI. Conclusions

In this paper, an accurate and computationally efficient procedure is given for the calculation of spatial Green's functions as the inverse Fourier transforms of their spectral equivalents. A general extraction technique is worked out to handle the asymptotic and singular behavior of the Green's functions in the case of an arbitrary stratified dielectric medium. The asymptotic extraction leads to analytical functions, which describe the singular behavior at the origin of the spatial functions. The singular behavior around poles and branch point are both annihilated using new subtraction functions. These new functions give rise to analytical expressions for the Green's functions at larger distances. Some very interesting characteristics of these functions are proven that can be exploited in mutual coupling calculations. A simple but fast technique is given for the numerical integration of well-behaved integrands. The efficiency of the procedure is discussed and illustrated. The accuracy can be checked through comparison between calculated and measured results published in earlier papers and in the second part of this paper. In our view, the main advantages of the proposed procedure are its generality, its relative simplicity, the possibility to implement it in a straightforward way in the case of multilayered structures (even if the number of layers is not known in advance), its special design to be used in cases where a large number of Green's functions is needed, and definitely the property that every spatial Green's function evaluated not too close to the source can be approximated as set of waves of which the characteristics offer some opportunities to be used in part two of the paper.

Appendix
Characteristics of the Space Wave in a Multilayered Structure

Every Green's function $g_F(\beta, z)$ (F equals V or I depending on the field component) can be expanded in series around $\gamma = 0$

$$g_F(z) = A_{-1}^F(z)\frac{1}{\gamma} + A_0^F(z)\frac{1}{K} + A_1^F(z)\frac{\gamma}{K^2} + A_2^F(z)\frac{\gamma^2}{K^3} + \cdots, \qquad \beta \simeq K \tag{26}$$

with $A_{-1}^F(z) = \lim_{\gamma\to 0} \gamma g_F(\beta, z)$ and $A_1^F(z) = \lim_{\gamma\to 0} \frac{K^2}{2}\frac{d^2}{d\gamma^2}(\gamma g_F(\beta, z))$. In each layer i, the Green's function follows the transmission line equation derived from (2) and (3)

$$\frac{d^2}{dz^2} g_F(\beta, z) - \gamma_i^2 g_F(\beta, z) = 0. \tag{27}$$

Inserting (26) in (27), multiplying with γ and taking the limit for $\gamma \to 0$ yields

$$\frac{d^2}{dz^2} A_{-1}^F(z) - (K^2 - k_i^2) A_{-1}^F(z) = 0. \tag{28}$$

The sources are unit sources independent of β and, consequently, there are no contributions proportional to $1/\gamma$ or γ. Thus, $A_{-1}^F(z)$ is the solution of a source-free transmission line problem. Consequently, the z dependence of $A_{-1}^F(z)$ given by $C^{F,K,-0.5}(z)$ will be unique for each source in the multilayered structure independent of its type—magnetic or electric—or its position.

To determine $A_1^F(z)$, (26) is inserted in (27). The latter is multiplied by $K^2\gamma/2$ and the limit for $\gamma \to 0$ of the second derivative with respect to γ is calculated, resulting in

$$\frac{d^2}{dz^2}\left(A_1^F(z)\right) - \lim_{\gamma\to 0}\left(\gamma_i^2\right) A_1^F(z) - \lim_{\gamma\to 0}\left(\frac{d^2}{d\gamma^2}\left(\frac{1}{2}\gamma_i^2\right)\right) K^2 A_{-1}^F(z) - \lim_{\gamma\to 0}\left(\frac{d}{d\gamma}\left(\gamma_i^2\right)\right) K A_0^F(z) = 0. \tag{29}$$

One can verify that $\lim_{\gamma\to 0}\left(\gamma_i^2\right) = K^2 - k_i^2$, $\lim_{\gamma\to 0}\left(\frac{d}{d\gamma}(\gamma_i^2)\right) = 0$ and $\lim_{\gamma\to 0}\left(\frac{d^2}{d\gamma^2}(\frac{1}{2}\gamma_i^2)\right) = 1$.

In a nonhomogeneous multilayered structure, one can prove that $A_{-1}^F(z) = 0$. The singular behavior around the branch point is determined by $A_1^F(z)$, which is again a solution of the source-free transmission line equations. The same conclusion can be drawn for this function.

In a homogeneous structure (backed by a conducting plate), the situation is a bit different. In the TE system, $A_{-1}^F(z) = 0$ for either an electric or magnetic field Green's function. In the TM system, $A_{-1}^I(z)$ is different from zero. Making use of (2) and (3) for a homogeneous structure and the boundary condition at the ground plate $V(\beta, z \text{ at ground plate}) = 0$, it can be verified that

$$A_{-1}^I(z) = C_1 \text{ and } A_{-1}^V(z) = 0 \tag{30}$$

and

$$A_1^I(z) = C_2 + C_1 \frac{z^2}{2} \quad \text{and}$$
$$A_1^V(z) = 0 - C_1 \frac{z}{j\omega\epsilon} \tag{31}$$

if $z = 0$ at the ground plate. Those functions can also be found as the limit for $\gamma_p \rightarrow 0$ of a quasi-homogeneous structure.

REFERENCES

[1] G. A. E. Vandenbosch and A. R. Van de Capelle, "Mixed-potential integral expression formulation of the electric field in a stratified dielectric medium—Application to the case of a probe current source," *IEEE Trans. Antennas Propagat.*, vol. 40, pp. 806–817, July 1992.

[2] T. Itoh, "Spectral domain immitance approach for dispersion characteristics of generalized printed transmission lines," *IEEE Trans. Microwave Theory Tech.*, vol. MTT-28, pp. 733–736, July 1980.

[3] A. K. Bhattacharyya, "Characteristics of space and surface waves in a multilayered structure," *IEEE Trans. Antennas Propagat.*, vol. 38, pp. 1231–1238, Aug. 1990.

[4] P. B. Katehi and N. G. Alexopoulos, "Real axis integration of Sommerfeld integrals with applications to printed circuit antennas," *J. Math. Phys.*, vol. 24, pp. 527–533, Mar. 1983.

[5] J. R. Mosig and T. K. Sarkar, "Comparison of quasistatic and exact electromagnetic fields from a horizontal electric dipole above a lossy dielectric backed by an imperfect ground plane," *IEEE Trans. Microwave Theory Tech.*, vol. MTT-34, pp. 379–387, Apr. 1986.

[6] K. A. Michalski and D. Zheng, "Electromagnetic scattering and radiation by surfaces of arbitrary shape in layered media, part II: Implementation and results for contiguous half-spaces," *IEEE Trans. Antennas Propagat.*, vol. 38, pp. 345–352, Mar. 1990.

[7] J. R. Mosig and F. E. Gardiol, "Analytical and numerical techniques in the Green's functions treatment of microstrip antennas and scatterers," *Proc. Inst. Elect. Eng.*, vol. 130, pt. H, pp. 175–182, Mar. 1983.

[8] H.-Y. Yang, A. Nakatani, and J. A. Castaneda, "Efficient evaluation of spectral integrals in the moment method solution of microstrip antennas and circuits," *IEEE Trans. Antennas Propagat.*, vol. 38, pp. 1127–1130, July 1990.

[9] D. M. Pozar, "Input impedance and mutual coupling of rectangular microstrip antennas," *IEEE Trans. Antennas Propagat.*, vol. AP-30, pp. 1191–1196, Nov. 1982.

[10] ——, "Finite phased arrays of rectangular microstrip patches," *IEEE Trans. Antennas Propagat.*, vol. AP-34, pp. 658–665, May 1986.

[11] G. A. E. Vandenbosch and A. R. Van de Capelle, "Use of a combined expansion scheme to analyze microstrip antennas with the method of moments," *Radio Sci.*, vol. 27, pp. 911–916, Nov./Dec. 1992.

[12] S. Barkeshli, P. H. Pathak, and M. Marin, "An asymptotic closed-form microstrip surface Green's function for the efficient moment method analysis of mutual coupling in microstrip antennas," *IEEE Trans. Antennas Propagat.*, vol. 38, pp. 1374–1383, Sept. 1990.

[13] M. A. Marin and P. H. Pathak, "An asymptotic closed-form representation for the grounded double-layer surface Green's function," *IEEE Trans. Antennas Propagat.*, vol. 40, pp. 1357–1366, Nov. 1992.

Filip J. Demuynck (S'92–M'95) was born in Brugge, Belgium, on May 23, 1967. He received the M.S. and Ph.D. degrees in electrical engineering from the Katholieke Universiteit Leuven, Leuven, Belgium, in 1990 and 1995, respectively.

He was a Postdoctoral Researcher at the Katholieke Universiteit Leuven until January 1996, after which he worked for Alcatel Telecom. In July 1996, he joined the HP-EEsof Division of Hewlett-Packard, Ghent, Belgium, as an R&D Engineer working on the development of planar electromagnetic simulators. His interests include electromagnetics, numerical techniques, and the modeling of large circuits and antennas.

Guy A. E. Vandenbosch (M'92) was born in Sint-Niklaas, Belgium, on May 4, 1962. He received the M.S. and Ph.D. degrees in electrical engineering from the Katholieke Universiteit Leuven, Leuven, Belgium, in 1985 and 1991, respectively.

He was a Research and Teaching Assistant from 1985 to 1991 with the Telecommunications and Microwaves Section of the Katholieke Universiteit Leuven, where he worked on the modeling of microstrip antennas with the integral equation technique. From 1991 to 1993, he held a Postdoctoral Research Position at the Katholieke Universiteit Leuven. He is currently a Professor at the same university. His work has been published in a number of articles in international journals and has been presented at several conferences. His research interests are mainly in the area of computational electromagnetics, planar antennas and circuits, and electromagnetic compatibility.

Antoine R. Van de Capelle (S'70–M'84) was born in Nazareth, Belgium, in 1946. He received the M.Sc., Ph.D., and Special Doctors degrees from the Katholieke Universiteit Leuven, Belgium, in 1970, 1973, and 1979, respectively.

In 1970, he joined the Department of Electrical Engineering of the Katholieke Universiteit Leuven, where he is now a Professor. In 1974 he established a research group on antennas, which has done a lot of work on microstrip antennas. As a Professor at the Katholieke Universiteit Leuven, he teaches courses on telecommunication systems, electromagnetic waves, and antennas and radio propagation. His current research activities involve radio c wave circuits.